

The ultra-diffuse galaxy AGC 114905 needs dark matter

J. A. Sellwood^{1*} and R. H. Sanders^{2†}

¹*Steward Observatory, University of Arizona, 933 N Cherry Ave, Tucson AZ 85722, USA*

²*Kapteyn Astronomical Institute, P.O. Box 800, NL-9700 AV Groningen, the Netherlands*

26 April 2022

ABSTRACT

Recent 21 cm line observations of the ultra-diffuse galaxy AGC 114905 indicate a rotating disc largely supported against gravity by orbital motion, as usual. Remarkably, this study has revealed that the form and amplitude of the HI rotation curve is completely accounted for by the observed distribution of baryonic matter, stars and neutral gas, implying that no dark halo is required. It is surprising to find a DM-free galaxy for a number of reasons, one being that a bare Newtonian disk having low velocity dispersion would be expected to be unstable to both axi- and non-axisymmetric perturbations that would change the structure of the disc on a dynamical timescale, as has been known for decades. We present N -body simulations of the DM-free model, and one having a low-density DM halo, that confirm this expectation: the disc is chronically unstable to just such instabilities. Since it is unlikely that a galaxy that is observed to have a near-regular velocity pattern would be unstable, our finding calls into question the suggestion that the galaxy may lack, or have little, dark matter. We also show that if the inclination of this near face-on system has been substantially overestimated, the consequent increased amplitude of the rotation curve would accommodate a halo massive enough for the galaxy to be stable.

Key words: galaxies: spiral — galaxies: evolution — galaxies: structure — galaxies: kinematics and dynamics —

1 INTRODUCTION

Ultra diffuse galaxies (UDGs), which may comprise a distinct class of large galaxies having very low surface brightness (Impey *et al.* 1988; Conselice 2018), have recently attracted considerable attention. These objects are found in various environments ranging from large galaxy clusters to voids and may be gas-rich or gas free – facts that may indicate various formation and evolution mechanisms. Kinematic studies of at least one gas-free system have implied very low dynamical mass, consistent with the observed stellar mass, and it has been suggested that these systems may be entirely free of dark matter (van Dokkum *et al.* 2019).

More recently, 21 cm line studies of neutral hydrogen in several gas rich UDGs have revealed similar atypical properties (Mancera Piña *et al.* 2019): it appears that several do not lie on the well-established baryonic Tully-Fisher relation of brighter galaxies, in the sense that they are too slowly rotating for their observed baryonic mass. One particular galaxy, AGC 114905, is of comparable size to the Milky Way but has a rotational velocity a factor 10 times lower. This object has been studied in detail via 21 cm line observations by Mancera Piña *et al.* (2021, hereafter MP21). They fitted a differentially rotating inclined disc to the observed data cube, deriving a rotation curve that is apparently consistent with the attraction of the observed distribution of stars and

gas only. Basically, the detected baryonic matter, mostly gas which has no uncertainty in the stellar mass-to-light ratio, gives rise to a rotation curve that very closely matches that fitted to their data.

Disc galaxies that do not appear to be embedded in a dark matter halo would be remarkable for two principal reasons. First, the modern Λ CDM theory of galaxy formation (reviewed by Somerville & Davé 2015) supposes that galaxies form in pre-existing dark matter concentrations (but see also Moreno *et al.* 2022). Second, rotationally-supported galaxies lacking DM halos and a central bulge have long been known (Miller *et al.* 1971; Hohl 1971) to be globally unstable to the formation of a bar, which provided one of the original motivations for DM halos (Ostriker & Peebles 1973). The history of these issues is discussed in detail by Sanders (2010). Note that a DM free galaxy would also be clearly inconsistent with the MOND paradigm (Milgrom 1983) which requires every relatively isolated galaxy to have an apparent “halo”. These considerations account for the intense interest in UDGs.

Since a fully self-gravitating disc galaxy is expected to be globally unstable, we have constructed N -body realizations of the models of AGC 114905 fitted by MP21 to their data and evolved them to examine their stability. Full details of the models and our methods are given in the following section.

Implicit in the study presented here are the assumptions that the galaxy is undisturbed, in a long-lived state, and that the observed rotation pattern reflects centrifugal balance. Although the disc has not had many dynamical times to settle (the orbit period at the disc edge, $R = 10$ kpc, is ~ 3 Gyr),

* E-mail:sellwood@as.arizona.edu

† E-mail:sanders@astro.rug.nl

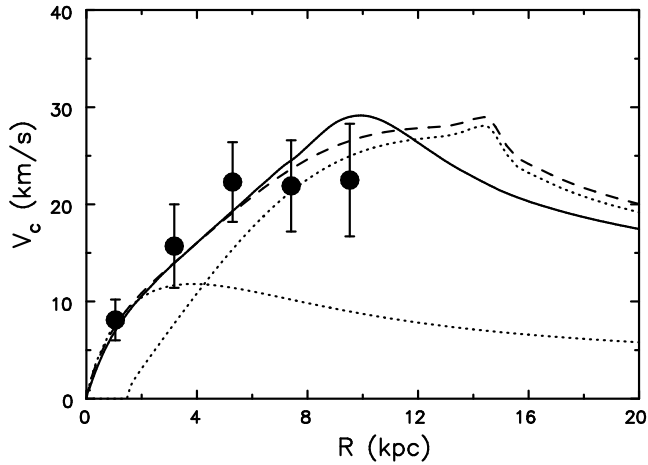


Figure 1. The data points with error bars show the circular speed in AGC 114905 measured by MP21 for an adopted inclination of 32° . The dashed curve to $R \lesssim 10$ kpc shows the circular speed in the no-DM model proposed by MP21 that is the sum, in quadrature, of the dotted curves, which are the contributions of the two disc components. The solid curve is the circular speed measured directly from the attachment of the particles in our simulation, see the text for more details. Note that the separate calculated rotation curves assume the surface density of the gas was tapered to zero near $R = 15$ kpc for the dashed curve and more gently and farther in for the solid curve. The solid and dashed curves are in good agreement inside $R \sim 8$ kpc, but the solid curve exceeds that expected from the extended gas disc for $8 \leq R \leq 10$ kpc.

the apparent regularity of the observed velocity field gives some credence to these assumptions but, were they not to hold, there is little that can be deduced from stability considerations.

2 TECHNIQUE

2.1 No DM model

Our first simulation is of a model without DM, whose properties are given in §4.1 of *Mancera Piña et al. (2021)*. These authors present neutral hydrogen observations of the galaxy from which they derive a deprojected circular speed that rises gently from zero at the centre to ~ 23 km s $^{-1}$ at $R = 10$ kpc.

MP21 fit the projected star light distribution as a round exponential disc and, adopting $M/L = 0.47$ in the r -band, give the surface mass density as

$$\Sigma_{\text{stars}}(R) = \frac{M_d}{2\pi R_d^2} \exp(-R/R_d). \quad (1)$$

Here $R_d = 1.79$ kpc is the disc scale length and $M_d = (1.3 \pm 0.3) \times 10^8 M_\odot$ is the mass of the notional infinite disc, the uncertainty reflecting that in the M/L . We taper the stellar disc surface density to zero over the range $3.5R_d \leq R \leq 4R_d$. There are no data (at the time of this writing) to indicate the stellar velocity dispersion in this galaxy, so we adopt $Q_{\text{stars}} \gtrsim 1.5$ (*Toomre 1964*). The Jeans equations in the epicyclic approximation (*Binney & Tremaine 2008*) are inadequate to construct a reasonable equilibrium for the star particles because the radial velocity dispersion is $\gtrsim 7$ km s $^{-1}$ near the disc centre which is comparable to the observed

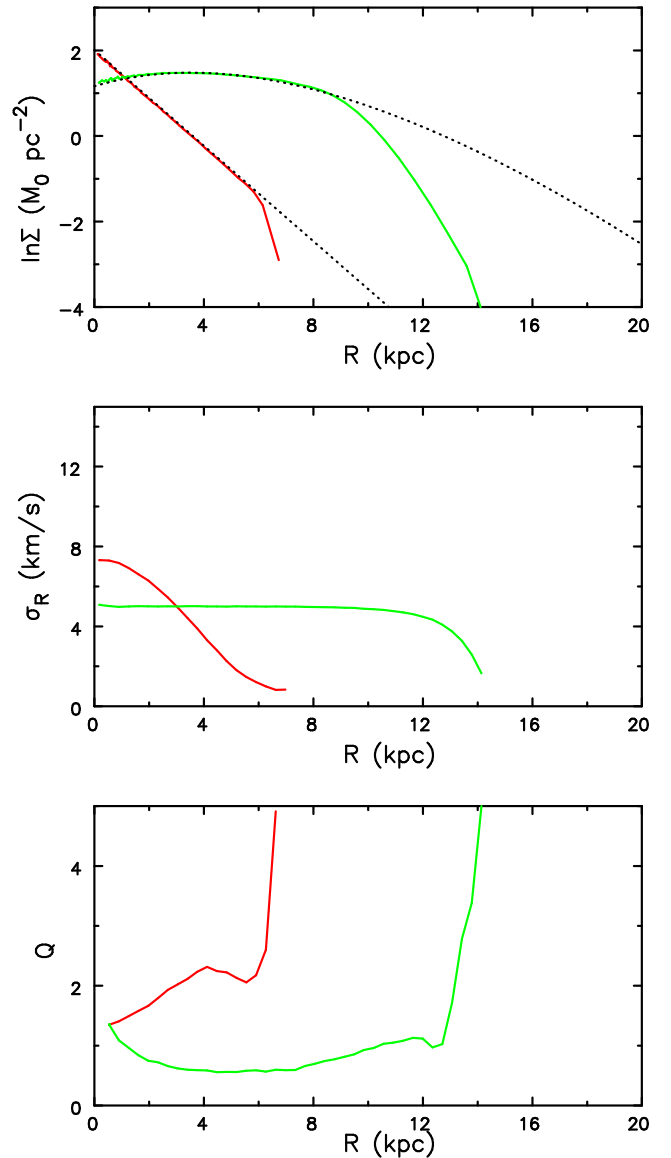


Figure 2. The solid lines in each panel are measured from the start of the no-DM matter simulation. The top panel shows the tapered surface densities of star particles (red) and of gas particles (green), while the dotted lines are the untapered functions (eqs. 1 and 2). The middle panel shows the radial velocity dispersion of the particles, while the bottom gives the stability parameter, Q , for each component.

circular speed. We therefore derive a 2D distribution function (DF) for the disc using the procedure described by *Shu (1969)*. As the vertical density profile of the disc is also unknown, we adopt a Gaussian profile with a scale $0.1R_d$, and use the 1D Jeans equation to set up the appropriate vertical velocity dispersion, which results in a slightly flattened velocity ellipsoid at all radii.

MP21 fit the observed gas surface density, corrected for helium content, with a function of the form

$$\Sigma_{\text{gas}}(R) = \Sigma_{0,\text{gas}} \exp(-R/R_1)(1 + R/R_2)^\alpha, \quad (2)$$

where the central surface density of the gas $\Sigma_{0,\text{gas}} = 3.2 M_\odot \text{ pc}^{-2}$, $R_1 = 1.11$ kpc, $R_2 = 16.5$ kpc, and $\alpha = 18.04$. The gas disc extends to $R \sim 10$ kpc, and has a total mass

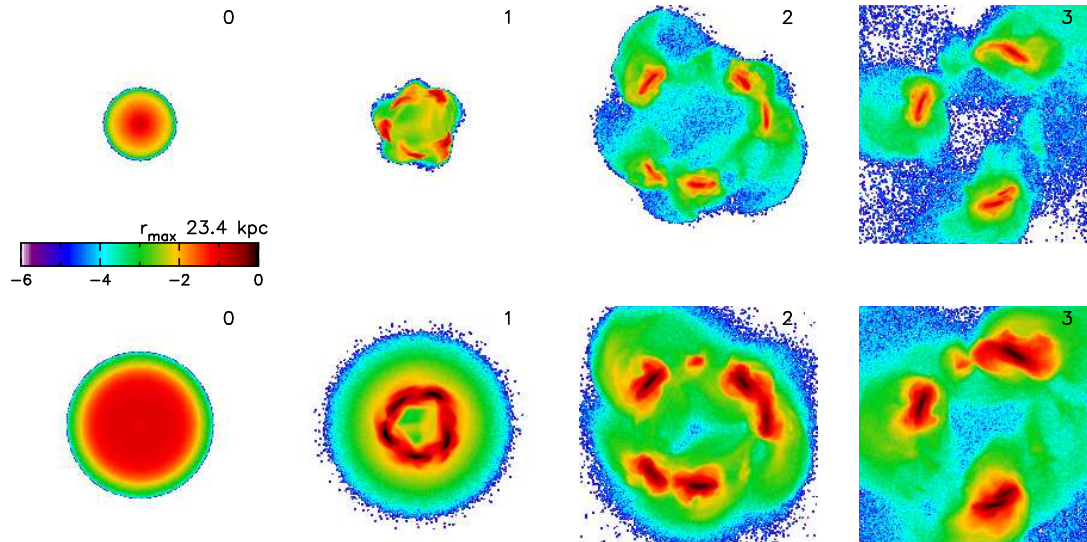


Figure 3. The evolution of the star component, top row, and gas component, bottom row, in the model with no dark matter. The colour scale indicates the logarithm of the projected particle density, times are in Gyr and the box is 46.8 kpc on a side.

Table 1. Default numerical parameters

| | |
|-------------------------------|----------------------------------|
| Grid points in (r, ϕ, z) | $175 \times 256 \times 125$ |
| Grid scaling | $R_d = 5$ grid units |
| Vertical spacing | $\delta z = 0.04 R_d$ |
| Active sectoral harmonics | $0 \leq m \leq 8$ |
| Softening length | $R_d/20$ |
| Number of star particles | 10^6 |
| Number of “gas” particles | 10^7 |
| Time-step | $(R_d^3/GM)^{1/2}/80 = 1.24$ Myr |

of $(1.29 \pm 0.19) \times 10^9 M_\odot$; it is therefore both more extensive and ten times more massive than the stellar disc. MP21 point out that the attraction of the two disc components gives rise to a rotation curve, the dashed line in Figure 1, that is in reasonable agreement with the observed velocities. MP21 measure the velocity dispersion of the gas component to be close to $\sim 5 \text{ km s}^{-1}$ at most radii and $\sim 8 \text{ km s}^{-1}$ at their innermost point. We adopt an approximately isotropic velocity dispersion of 5 km s^{-1} at all radii.

In most of our simulations, we model the gas disc as a collection of collisionless N -body particles, but we have tried the SPH option in GADGET-2 in one case (see §3.1).

Once again, we select “gas” particles from a 2D DF created by Shu’s procedure in order to build an equilibrium disc model, although in this case the outer edge of the disc presented an extra difficulty. The function (eq. 2) fitted to the disc surface density peaks near $R \sim 3$ kpc and declines gently to beyond $R = 10$ kpc with no outer truncation. As is well known (Toomre 1963; Casertano 1983), introducing a sharp truncation to a disc creates a blip in the central attraction, causing the circular speed to rise steeply to the truncation radius and to decline more quickly than the Keplerian rate just beyond. MP21 report that the observed circular speed stays flat over the last few measured points, as shown in Figure 1, revealing no kinematic signature that the gas disc has an edge, even though their Fig. 1 hints that the HI disc ends quite sharply near $R \sim 10$ kpc. We were told (Fraternali, private communication) that this apparent edge is probably an

artifact introduced by a mask in their data reduction procedure, and the gas disc may extend smoothly to larger radii.

Since there are no kinematic data for $R \gtrsim 10$ kpc, we prefer to truncate the gas disc, even though it creates a feature in the central attraction that is not observed. However, it is numerically inconvenient to find a DF and to select particles in a potential that causes a blip in the rotation curve near the disc edge. We therefore tapered the surface density of the gas disc over the radial range $10.7 < R < 14.3$ kpc in order to moderate the effect of truncation, although a broader and more gentle bump in the circular speed curve remains, as shown by the solid curve in Figure 1. In order to avoid numerical problems, we computed the DF and selected particles in a potential derived from a gas disc having the taper shifted to a larger radius, which made it easier to assign orbital velocities to the gas particles, although the actual surface density of the selected particles was tapered as noted above. The attraction in the outer disc ($8 \leq R \leq 10$ kpc) is stronger in the simulation (solid curve) than assumed when selecting particles from this DF (dashed curve), which causes the gas particles to have a somewhat lower orbital speed than needed for centrifugal balance. The disc inside 8 kpc, which contains most of the mass, is in proper equilibrium, and we do not expect the mild imbalance in the outer part, which causes a slight initial contraction, to affect the overall stability.

The tapered surface density profiles are shown in the top panel of Figure 2, and the other two panels present properties of this model measured from the particles at the start of the simulation. Note that Q_{gas} in the bottom panel, which is determined by the measured velocity dispersion, surface density, and rotation curve, is less than unity over a broad radial range.

2.2 Numerical methods

The particles in our simulations move in a 3D volume that is spanned by a cylindrical polar mesh. The self-gravitational attractions are calculated at grid points and interpolated to the position of each particle. A full description of our numeri-

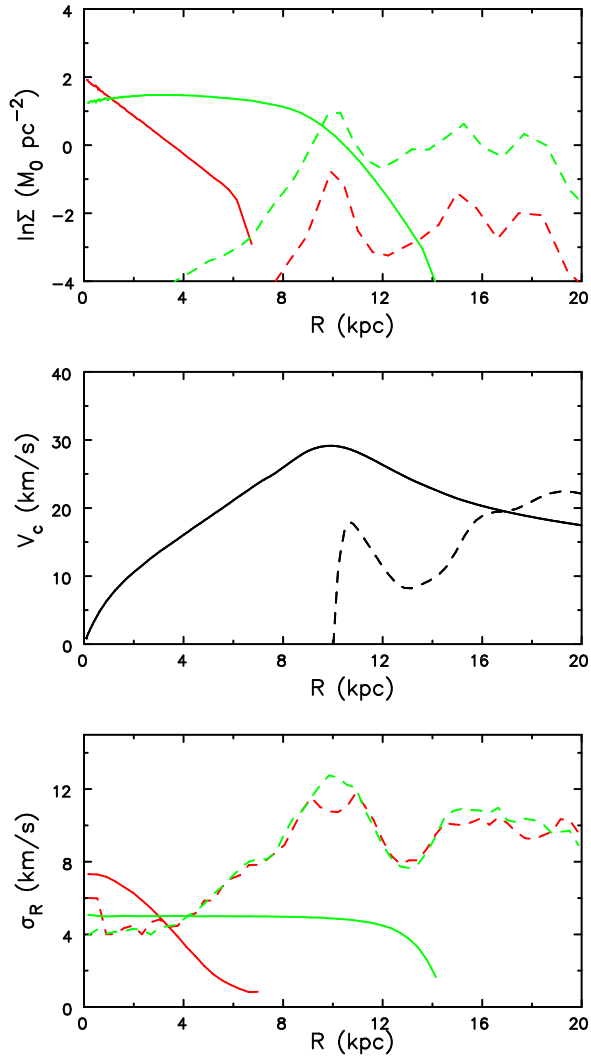


Figure 4. The initial (solid curves) and final (dashed curves) of the azimuthally averaged surface density (top panel) and radial velocity dispersion (bottom panel) in the model shown in Figure 3. The colours are red for stars and green for gas, as in Figure 2. The middle panel gives the initial and final rotation curves.

cal procedures is given in the on-line manual (Sellwood 2014) for the GALAXY code and the source is available for download. Table 1 gives the values of the numerical parameters adopted for the simulations presented in this paper.

We have verified that the results we obtain are insensitive to the numbers of particles employed, whether the particles are confined to a plane or move in 3D, and also when evolved using the N -body option of GADGET-2 (Springel 2005). We describe below (§3.1) the behaviour of a model in which we turned on SPH for the gas particles.

3 RESULTS

We evolved the model presented in §2.1 for 3 Gyr, and a few snapshots are shown in Fig. 3. The evolution of the stellar component is illustrated in the top row and the gas particles in the bottom row. The more massive gas component, which initially had $Q_{\text{gas}} < 1$ over a broad radial range (bot-

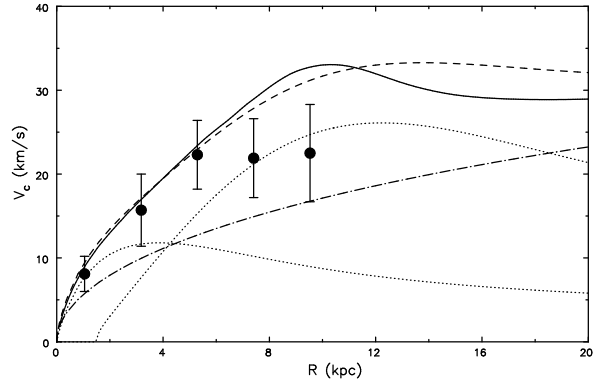


Figure 5. The initial rotation curve of the “Case 2” model having the low-concentration DM halo. The data points have been reproduced and the lines are the same as in Fig. 1, except that the dot-dashed line gives the contribution of the halo to the new total circular speed, marked by the dashed and solid curves.

tom panel of Fig. 2), and thus was axisymmetrically unstable (Toomre 1964), formed a ring at first which then fragmented. Note the stellar disc had $Q_{\text{stars}} > 1$ everywhere but the attraction of the gas particles caused it to behave in a similar manner.

Although the initial model was in equilibrium, the rapid growth of instabilities profoundly changed the structure of both discs, as shown in Figure 4. Both discs expanded leaving a very low central density (top panel) and, because angular momentum is conserved, the orbital speeds of the particles decreased, while random motion was greatly increased (bottom panel). We stopped the simulation when the rate of change of these properties was beginning to slow. The middle panel shows a “rotation curve” at the last moment that differs profoundly from that observed.

3.1 Gas physics

We resimulated this model using GADGET-2 initially as N -body particles, obtaining very similar results as with GALAXY. We then attempted to apply the SPH option of GADGET-2 for the gas component. In this case, we adopted an isothermal equation of state for the gas with a sound speed of 5 km s^{-1} and no star formation or feedback. We found that the gas disc began to fragment even more rapidly than when employed collisionless particles, and the gas clumps reached such a density that GADGET-2 stopped after just 0.24 Gyr. This well-known behaviour of dissipative gas with self-gravity may possibly be inhibited by allowing star formation and feedback but, while the galaxy has a blue colour ($g - r = 0.3 \pm 0.1$) (Mancera Piña *et al.* 2020; Gault *et al.* 2021), these authors did not note particularly vigorous star formation. We did not pursue this option in part for this reason, but also because we would not expect it to alter the conclusion that the model is globally unstable.

3.2 Including a dark matter halo

Although the observed velocities in AGC 114905 could be accounted for without including a DM component, MP21 noted that some dark matter content should be expected. They therefore presented two models that included dark matter

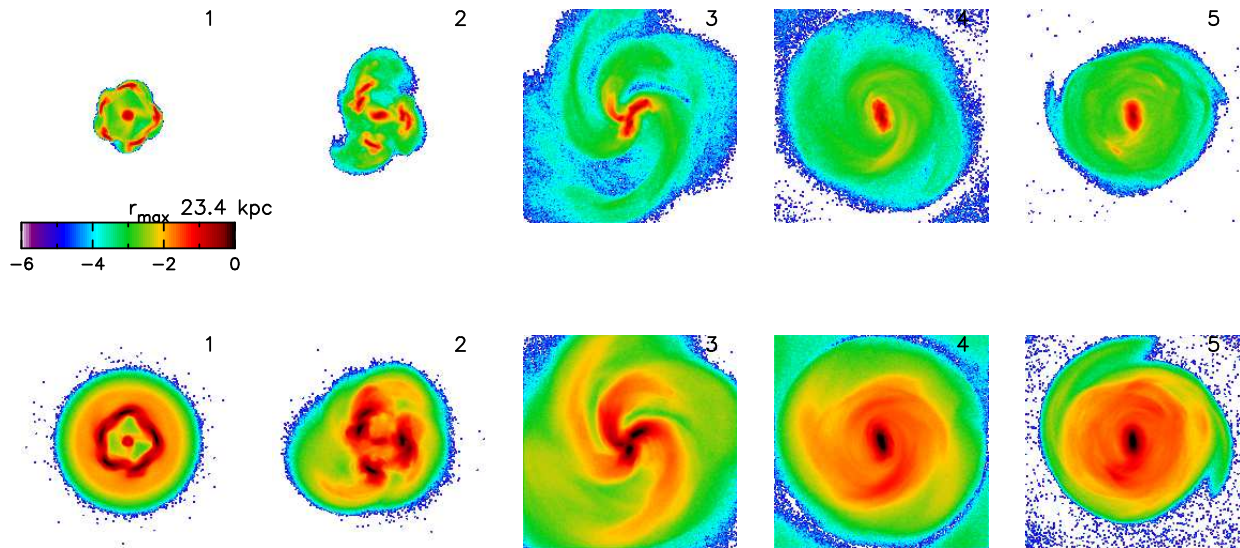


Figure 6. As for Fig. 3, but for the model having a low-concentration DM halo. Note that the times of the snapshots also differ.

halos having CORENFW (Read *et al.* 2016) density profiles. They restricted the allowed parameters of the halo to values in the cosmologically expected range in their Case 1, but were unable to fit circular speeds as low as observed. So they removed the restriction on the concentration parameter and present a model, their Case 2, that has $c = 0.3$. Adding a halo of mass $M_{200} = 10^{10} M_{\odot}$ and this low concentration, while retaining the previously fitted disc densities for the stars and gas, resulted in a rotation curve with higher amplitude, but perhaps consistent with their observed values within the errors, as shown Figure 5. MP21 acknowledge that the low concentration of this halo is well below the range expected for Λ CDM halos.

We have therefore created an N -body realization of the two-component disc in the rigid gravitational potential of their Case 2 DM halo component. The different gravitational field required us to rederive new DFs for both discs. We kept the properties of both discs as before, except that we thickened the gas layer in order that the vertical velocity dispersion was very similar to the 5 km s^{-1} assigned to the radial component to make the velocity ellipsoid more nearly isotropic. (Epicyclic motions require the azimuthal dispersion to differ from the radial component.) Since the circular speeds are higher, the epicyclic frequency is also increased by the DM halo, slightly raising the initial Q_{gas} , although it is still less than unity over the range $2 < R < 8 \text{ kpc}$.

The evolution of this model is presented in Figure 6. Since this simulation evolved more slowly and less violently, we ran it for longer. The evolution was also changed in other respects: an almost axisymmetric instability was again the first to develop, but non-axisymmetric features were already prominent by $t = 1 \text{ Gyr}$. The order of rotational symmetry of these features decreased over time and both the stellar and gas particles developed a bar by $t \sim 3 \text{ Gyr}$ that persisted to the end.

Figure 7 compares the initial and final properties of this model. The discs did not spread by quite as much (top panel) and their central densities rose rather than declined, unlike in first simulation, causing a profound change to the rotation curve (middle panel). The level of random motion was also

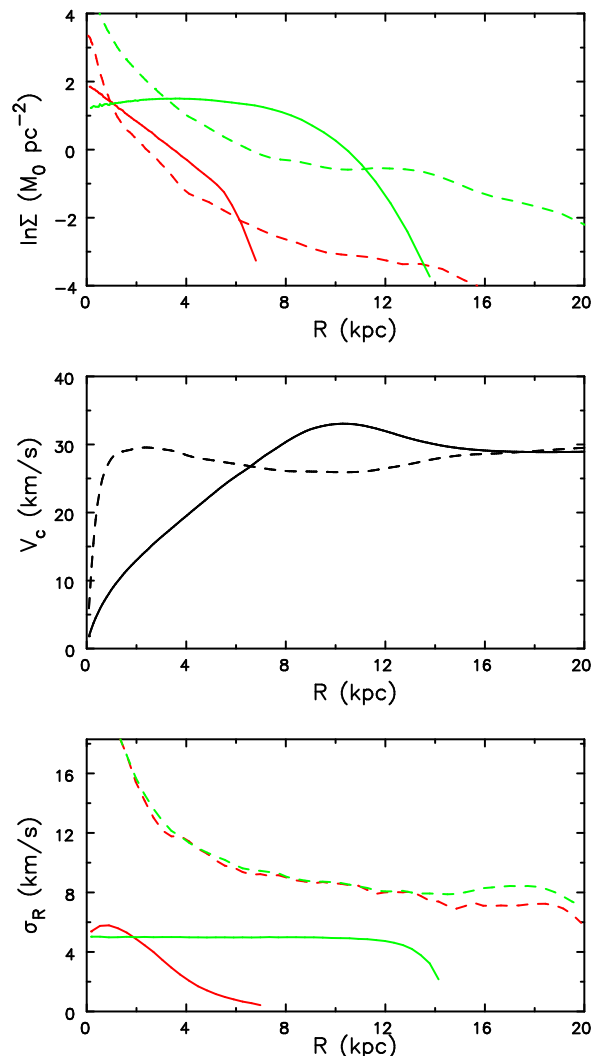


Figure 7. Same as Figure 4 but for the model shown in Figure 6.

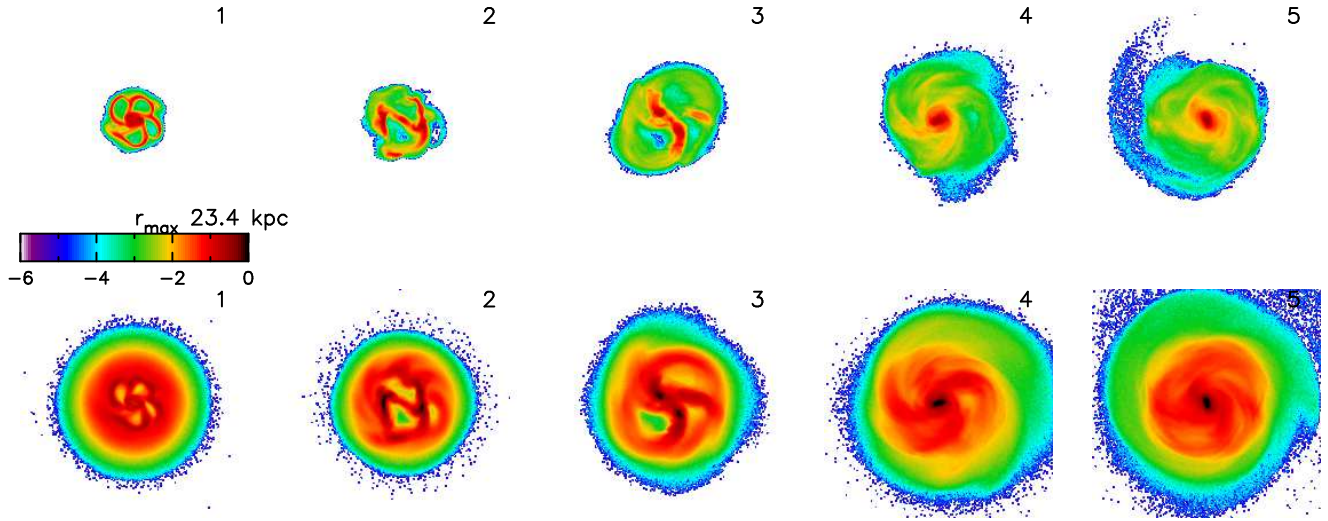


Figure 8. As for Fig. 3, but for a model in which we reduced the estimated inclination to 20° .

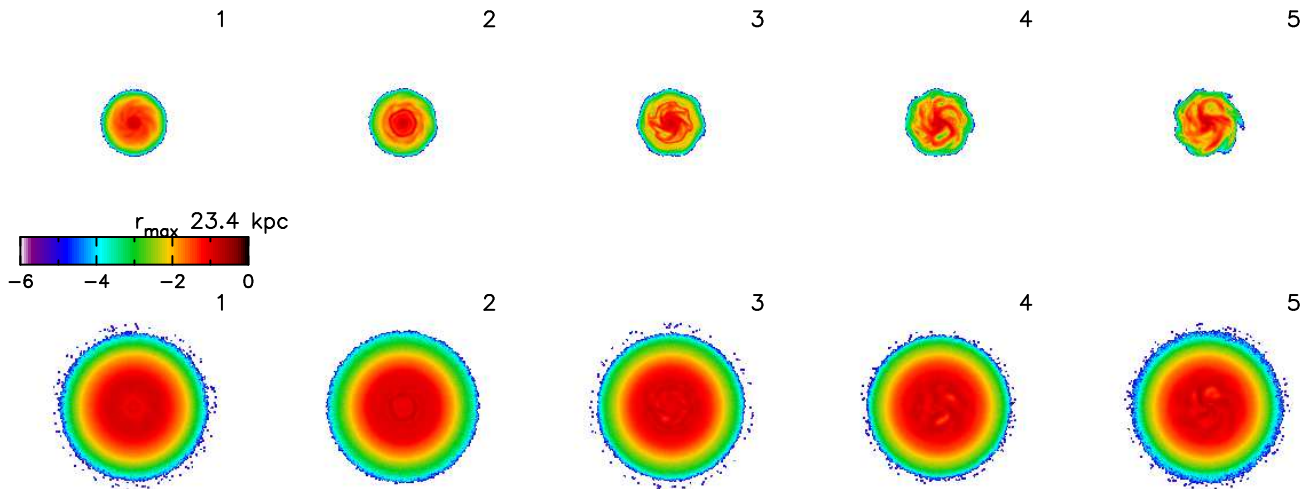


Figure 9. As for Fig. 8, but for the estimated inclination of 15° .

greatly increased by the end of the simulation (bottom panel). Once again, we consider these changes to be extensive enough to indicate that the initial model was unacceptable as a long-lived state.

We treated the DM halo in this simulation as a rigid component. Previous work (Athanasoula 2002; Sellwood 2016) has shown that realizing the halo with mobile particles causes the disc to be more unstable.

4 SEARCHING FOR A STABLE MODEL

The gas and stars in the galaxy AGC 114905 manifest some density variations, but it is very unlikely that MP21 observed it at a moment just before the discs disrupted due to instabilities. Therefore we have attempted to find a different stable, or slowly evolving model that matches their data. However, the stubborn fact is that the gas disc is alone massive enough to account for most of the inferred circular speed, and has

$Q < 1$ over a broad radial range. These properties inevitably imply instability.

Note $Q \equiv \sigma_R \kappa / (3.36 G \Sigma)$ (Toomre 1964), with κ being the usual epicyclic frequency (Binney & Tremaine 2008).¹ Thus Q could be higher if either σ_R has been underestimated, or the circular speed has been underestimated, implying a higher value for κ , or the surface density of the gas has been overestimated, or any combination of these factors.

MP21 report an HI mass, without correction for helium, of $M_{\text{HI}} = (9.7 \pm 1.4) \times 10^8 M_\odot$, which is lower than $M_{\text{HI}} \approx 1.3 \times 10^9 M_\odot$ implied by the ALFALFA flux; the difference can probably be ascribed to missing short baselines in the interferometric data. Thus these data would seem to preclude the idea that the tolerance in the HI mass may be consistent with a significantly lower surface density for the gas.

¹ We prefer this definition for a turbulent, clumpy gas rather than $Q \equiv c \kappa / (\pi G \Sigma)$ that applies to a smooth barotropic fluid having a sound speed c , but the difference is minor.

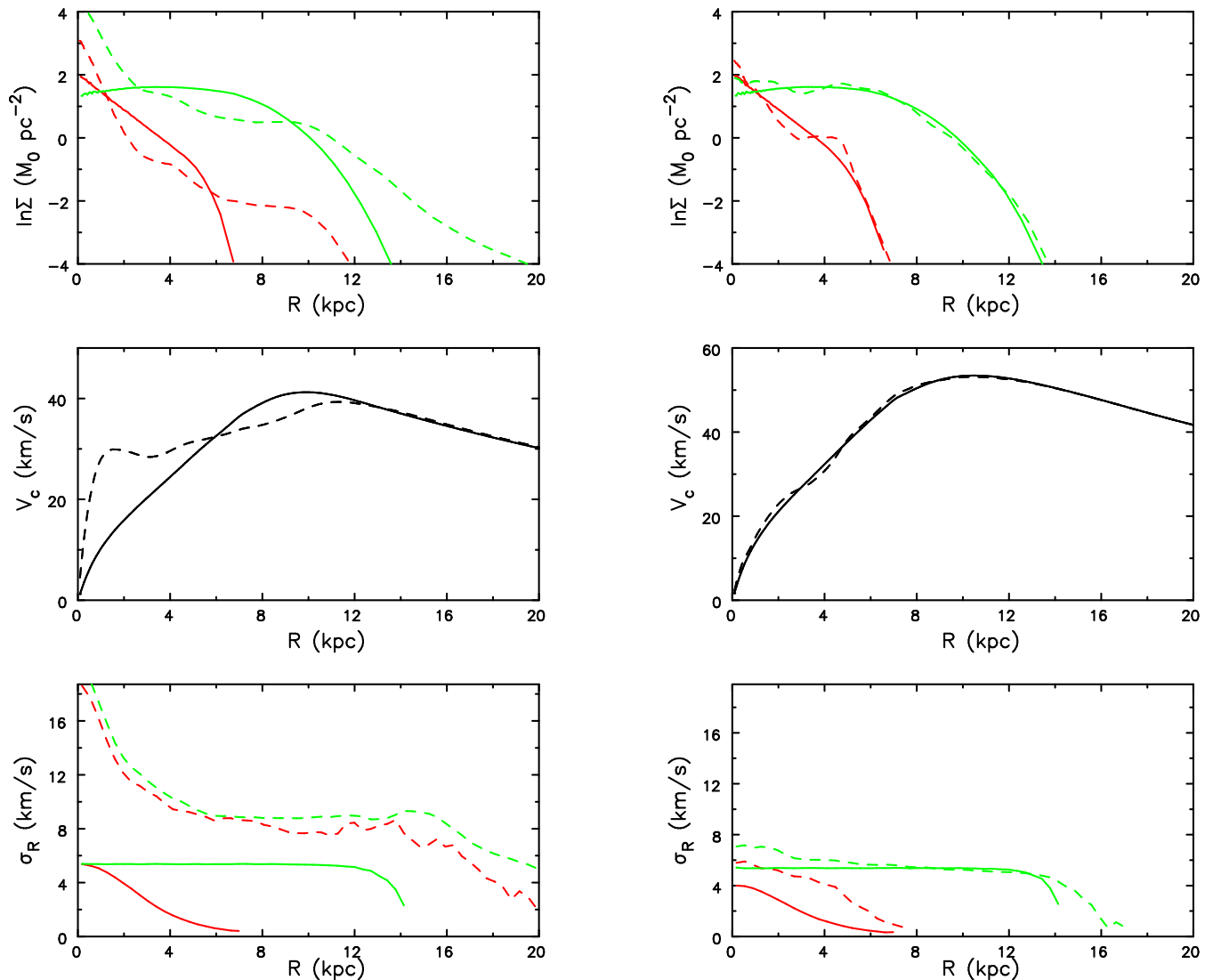


Figure 10. Same as Figure 4 but for the models shown in Figures 8 on the left and 9 on the right.

Although the stellar disc mass $M_* = (1.3 \pm 0.3) \times 10^8 M_\odot$ is less precisely known, its mass is merely $\sim 10\%$ of the mass of the gas disc and correspondingly less important to stability. We found that the evolution of a DM-free simulation was little affected by a $1\text{-}\sigma$ reduction in the mass of the stellar disc.

These considerations suggested two distinct strategies find stable, long-lived models.

4.1 Changing the disc inclination

One factor that could change the stability is a reduction to the adopted inclination of the disc, which is difficult to determine when the galaxy is close to face on. If it were in fact lower than the $\sim 30^\circ$ preferred by MP21 the rotation curve amplitude would be higher, which would in turn allow a more massive halo, as MP21 note in their §5.4. We have therefore tried a series of simulations to find the maximum inclination at which the stellar and gas discs, having the properties described in §2 above, would be stable, or slowly evolving.

We do not need to construct a halo model to make these tests, since we can add to the radial forces from the particles the central attraction of whatever rigid mass is needed to account for the difference between the rotation curve that arises from the baryonic matter, which we already know, and the scaled up rotation curve. The radial density profile of this implied halo has a uniform core inside ~ 100 pc and the density declines as $r^{-\alpha}$ over the range $2 < r < 8$ kpc, with $\alpha \sim 0.9$. This is quite different from the profile expected in Λ CDM galaxy formation theory.

Figures 8 & 9 present the results from two simulations in which we allowed higher circular speeds through supposing the inclination to have been overestimated. Figure 8 shows the effect of increasing the circular speed shown in Fig. 1 by a factor of 1.5, which implies an inclination of $i \sim 20^\circ$ instead of $i \sim 30^\circ$ preferred by MP21. Since the contributions from the stellar and gaseous discs are unchanged, and the rotation curve is simply scaled up, the implied DM mass to $R \sim 10$ kpc is 1.23 times the combined masses of the two discs. As may be seen, this DM component weakens the instabilities in the two discs, although they continued

to develop; a bar formed after 4 Gyr, which weakened by $t \sim 5$ Gyr.

The final properties of this model are shown in the left-hand panels of Figure 10. The changes in density (top panel) and velocity dispersion (bottom panel) resemble those in Figure 7, and the changes occurred over a similar time period. The middle panel reveals that the change to the rotation curve is a little less significant than in Figure 7, probably because of the substantial contribution from the rigid halo.

We doubled the amplitude of the rotation curve for the simulation shown in Figure 9, implying an inclination of the galaxy $i \sim 15^\circ$ and a DM halo mass 2.9 times the combined mass of the two discs inside $R \sim 10$ kpc. In this case, neither disc evolved significantly as shown in the right-hand panels of Figure 10 and the rotation curve was little changed by the end.

From these results, we learn that the apparently puzzling instability of the Case 2 model for AGC 114905 proposed by MP21, goes away if the inclination of the galaxy to the line of sight is reduced from their adopted $i \approx 30^\circ$ to $\sim 15^\circ$. The higher circular speed in this model allows room for a DM mass ~ 3 times the combined baryonic mass of the stellar and gaseous discs, thereby slowing the evolution and removing the challenge presented by their model. If the true inclination were in the range $10^\circ \lesssim i \lesssim 12^\circ$, this object would place clearly on the baryonic Tully-Fisher relation (McGaugh 2009).

MP21 determine the inclination of the disc in AGC 114905 from the apparent ellipticity of the gas disc, which they assume to be intrinsically round. Decreasing their fitted value of $i = 32^\circ$ therefore implies that the gas disc may be mildly *non-axisymmetric*. Indeed, the map of the HI surface density (Mancera Piña *et al.* 2021, their Fig. 1) shows some evidence of this; the axis ratio of the surface density contours is not constant and appears to change position angle with radius. This is not consistent with an axisymmetric disc seen in projection. Deeper HI observations of this, and of other gas-rich UDGs, may shed further light on this issue.

4.2 Stretching the data

Rather than pinning all the blame on a error in the estimated inclination, Pavel Mancera Piña and Filippo Fraternali (private communication, 2022), suggested that all the observational uncertainties may have conspired together to favour instability, and that a stable model could be consistent with the data, within the measured uncertainties. They therefore asked us to examine the stability of a model with a CORENFW halo that was more massive than that in their Case 2 model that we examined above (Figures 6 and 7).

To construct their new model, which we refer to as Case 3, they first reduced the estimated distance to AGC 114905 from 76 Mpc to 66 Mpc, a $2\text{-}\sigma$ change, that reduced the masses, and sizes, of the discs. They also reduced the M/L of the stars by $1\text{-}\sigma$. The new discs have the same functional forms as given in equations 1 and 2, but with revised values of the parameters: $\Sigma_{0,\text{stars}} = 6.3 M_\odot/\text{pc}^{-2}$ and $R_d = 1.35$ kpc for the stellar disc and $\Sigma_{0,\text{gas}} = 3.4 M_\odot/\text{pc}^{-2}$ and $R_1 = 1.00$ kpc, $R_2 = 14.82$ kpc, with unchanged $\alpha = 18.04$ for the gas disc. The mass of the stellar disc is $10^8 M_\odot$ and the gas mass inside 10 kpc is $1.04 \times 10^9 M_\odot$. They also reduced the inclination by $2\text{-}\sigma$ to 26° , and included the most massive halo that would not cause the circular speed to exceed the observed values by

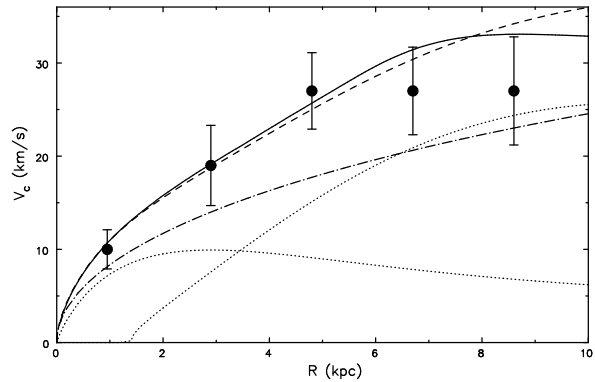


Figure 11. The initial rotation curve of Case 3, the model described in §4.2 in which the parameters have been stretched. The lines are the same as for Case 2 in Fig. 5, and the observed circular speeds with error bars have been changed from those above to reflect the revised inclination and distance.

more than twice the measured uncertainty. The parameters of the CORENFW halo they adopt are: $M_{200} = 10^{10.45} M_\odot$, $c_{200} = 0.8$, $n = 0.05$, and $r_c = 4.59$ kpc.

They finally suggested that the velocity dispersion in the gas could be raised within the tolerances of their measurements, although they concede that the low signal-to-noise of their data makes the dispersion, and especially its uncertainty, difficult to estimate. We have therefore treated it as a free parameter and run three separate models with $\sigma_{\text{gas}} = 5, 8, \text{ and } 11 \text{ km s}^{-1}$ at all radii. Note that we also made corresponding changes to the thickness of the gas layer in order to keep a roughly isotropic distribution of the velocities for the gas in each case.

We adopted a standard NFW halo with $M_{200} = 10^{10.45} M_\odot$ and $c_{200} = 0.8$, and also kept the tapers of surface density the same in disc scale lengths as before, so that our realizations of their Case 3 model did not have exactly the rotation curve they proposed. Our model is shown in Figure 11, and compared with the measured circular speeds, which have been adjusted for the revised inclination and distance. The DM mass enclosed within 10 kpc is $1.40 \times 10^9 M_\odot$, which exceeds the total baryonic mass, $1.14 \times 10^9 M_\odot$, interior to that radius.

Simulations of these three realizations revealed that the models scarcely evolved when $\sigma_{\text{gas}} = 8$ or 11 km s^{-1} , but that with $\sigma_{\text{gas}} = 5 \text{ km s}^{-1}$ was unstable and evolved similarly to the ‘‘Case 2’’ model shown in Figure 6. The changes to the properties of the coolest of our Case 3 models are reported in Figure 12; the other two models scarcely evolved.

It is interesting to note that the minimum value of $Q_{\text{gas}} \sim 0.15\sigma_{\text{gas}}$ in these models, with σ_{gas} in km s^{-1} . Thus, the minimum $Q_{\text{gas}} > 0.75, 1.2$ and 1.7 for the three values σ_{gas} we have tried, and that only the model with $Q_{\text{gas}} < 1$ at some radii was unstable. Furthermore, the models of §4.1 for which we reduced the inclination had $Q_{\text{gas}} > 1$ everywhere only when $i \sim 15^\circ$, which also happened to be the only stable model. A possible inference from these results is that global instability is triggered when $Q_{\text{gas}} < 1$ somewhere in the disc.

Of course, $Q_{\text{gas}} \gtrsim 1$ everywhere is not a sufficient condition for stability – a significant halo mass is also required. In fact, increasing the velocity dispersion in the gas component of the no-halo model in §3 did not stabilize the disc; it formed

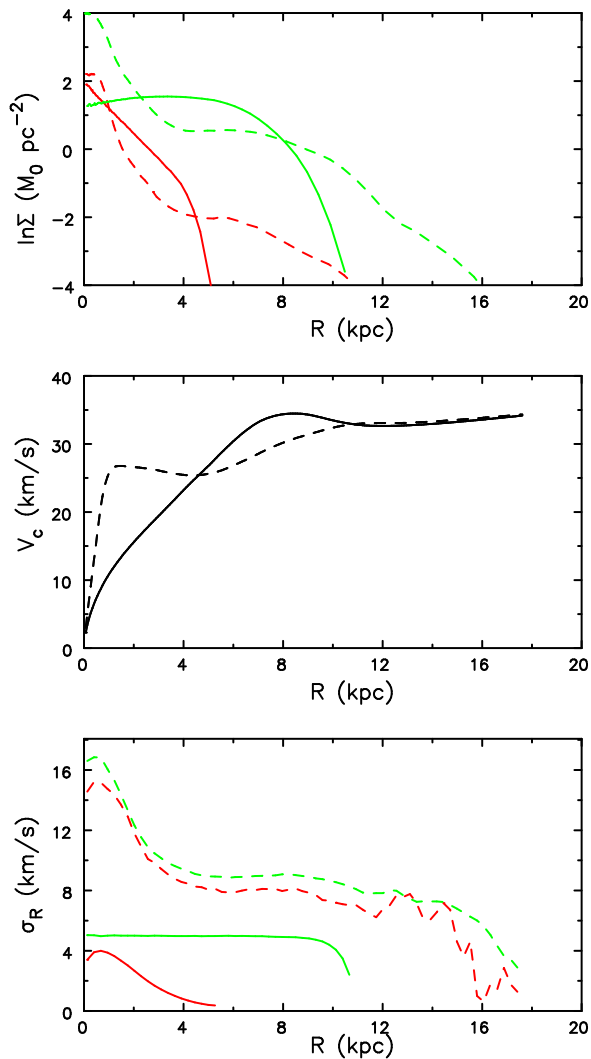


Figure 12. Same as Figure 4 but for Case 3 with $\sigma_{\text{gas}} = 5 \text{ km s}^{-1}$, showing that the model is unstable. Simulations having the same mass distribution but $\sigma_{\text{gas}} \geq 8 \text{ km s}^{-1}$ were stable.

a strong bar instead as expected from the earlier simulations by Hohl (1971), Ostriker & Peebles (1973) and analysis by Kalnajs (1978).

5 CONCLUSIONS

Rotationally-supported galaxy discs have long been known to be susceptible to various instabilities. The classic study by Toomre (1964) determined the $Q \geq 1$ criterion for axisymmetric stability, which has not needed significant subsequent revision. Although the mechanism for bar-forming instabilities (Hohl 1971; Kalnajs 1978; Sanders 2010) is now understood (Toomre 1981; Binney & Tremaine 2008), no general stability criterion is known and there are galaxies, such as M33, whose global stability remains a puzzle (Sellwood *et al.* 2019).

At face value, the properties of AGC 114905 measured by MP21 are extraordinary in *two* respects. Not only did they find that the attraction from the baryonic matter, stars and gas, could alone account for the centrifugal balance of the

disc, but their measurements also seemed to require that $Q \ll 1$ over a significant radial range. These properties suggest that both axisymmetric and bar-forming instabilities would be unavoidable, and our simulations have confirmed that a disc model having these properties disrupts violently on a dynamical time scale.

At the distance and inclination of the disc favoured by MP21, the orbit period at their outermost measured point is $\sim 3 \text{ Gyr}$, or $\gtrsim 20\%$ of the Hubble time, although it is shorter if the galaxy is closer and/or the inclination has been overestimated. Such a long dynamical time raises the possibility that the gas disc may not be relaxed or in centrifugal balance, and calls into question the validity of any mass modelling and conclusions from stability properties. However, MP21 observed an ordered flow pattern in the gas, which does suggest that the galaxy is both in a settled dynamical state and not subject to violently disruptive instabilities.

The standard method to stabilize a disc (Ostriker & Peebles 1973) is to embed it in a DM halo, and we have conducted simulations to confirm that this galaxy is stabilized by a large fraction of dark matter. The mechanism by which this works for both axisymmetric and bar-forming instabilities is to raise the epicyclic frequency, causing material in the disc to be more strongly tied to its home radius so that large-scale instabilities are thereby inhibited. Our simulations reported in §4.2 found that not only did the DM mass fraction have to exceed the baryonic mass, but that stability was not achieved unless $Q > 1$ everywhere also, which required the velocity dispersion of the gas to be significantly higher than that estimated by MP21. If the gas velocity dispersion were held at the observed value, we found in §4.1 an even larger DM mass fraction, ~ 3 times the baryon mass, was needed for stability.

However, these solutions do not fit comfortably with the findings of MP21. They converted their observed orbital speeds in projection, $V \sin i$, where V is the speed in the plane, by adopting an inclination $i \sim 32^\circ$ of the disc plane to the line of sight, which they estimated from the projected shape of the gas disc. It is well known that it is difficult to estimate the true value of i when the disc is this close to face on. Thus we considered models having a significantly decreased value for i , which increased the deprojected circular speed and allowed sufficient dark matter to stabilize the disc.

One can also imagine that the gas velocity dispersion, σ_{gas} , has been underestimated. The authors of MP21 concede (private communication) that it is hard to measure the gas velocity dispersion in their low S/N data and the value could exceed the $\sigma_{\text{gas}} \sim 5 \text{ km s}^{-1}$ they gave in their paper. However, the outer discs of large galaxies, beyond R_{25} , have velocity dispersions in the gas of $5\text{--}7 \text{ km s}^{-1}$ (Kamphuis 1993; Tamburro *et al.* 2009). This consideration leads us to prefer $\sigma_{\text{gas}} \simeq 5 \text{ km s}^{-1}$ in AGC 114905, and therefore a lower value for i ($\sim 15^\circ$) is needed for this one galaxy to be stable.

One possible cause of an overestimated inclination could be that the disc is, in fact, non-axisymmetric. The sample of UDGs from which MP21 chose AGC 114905 have low inclinations in general, and the estimated inclination is very sensitive to mild oval distortions of the disc. For low inclination systems an intrinsic non-axisymmetric shape generally biases the estimated inclination to higher values (*e.g.* Li *et al.* 2018, last panel of their Fig. 3).

All these objects are known to have low surface density

and a gas disc that is more massive and extensive than the stellar disc, although MP21 currently have sufficient information to determine the rotation curve and the value of Q in AGC 114905 only. The stability of this class of galaxies would be more difficult to understand if other UDGs in their sample also turned out to be apparently unstable. It is possible that such objects are intrinsically non-axisymmetric because of the sort of instabilities considered here. On the other hand it may be best not to attach much significance to models of discs having inclinations less than 40° , as has been traditional in rotation curve studies.

ACKNOWLEDGEMENTS

We thank both Filippo Fraternali and Pavel Mancera Piña for valuable comments on our results, suggestions for new tests, and for being helpfully engaged with our project throughout. We are also grateful to Moti Milgrom for very useful comments on the role of inclination in biasing the Tully-Fisher relation. JAS acknowledges the continuing hospitality of Steward Observatory.

DATA AVAILABILITY

The data from the simulations reported here can be made available on request. The simulation code can be downloaded from <http://www.physics.rutgers.edu/galaxy>

REFERENCES

- Athanassoula, E. 2002, ApJ, **569**, L83-L86
 Binney J. & Tremaine S. 2008, *Galactic Dynamics* 2nd ed. (Princeton University Press, Princeton NJ)
 Casertano, S. 1983, MNRAS, **203**, 735
 Conselice C.J. 2018, Research Notes of the American Astronomical Society, **7**, 43
 Gault, L., Leisman, L., Adams, E. A. K., *et al.* 2021, apj, **909**, 19
 Hohl, F. 1971, ApJ, **168**, 343
 Impey C., Bothun G. & Malin D. 1988, ApJ, **330**, 634
 Kalnajs, A. J. 1978, in IAU Symposium **77 Structure and Properties of Nearby Galaxies** eds. E. M. Berkhuisjen & R. Wielebinski (Dordrecht:Reidel) p. 113
 Kamphuis, J. 1993, PhD thesis., University of Groningen
 Li, P., Lelli, F., McGaugh, S., Schombert J. 2018, A&A, **615**, A3.
 Mancera Piña, P., Fraternali, F., Adams, E.A., *et al.* 2019, ApJ, **883**, L33
 Mancera Piña, P. E., Fraternali, F., Oman, K. A., *et al.* 2020, MNRAS, **495**, 3636
 Mancera Piña, P., Fraternali, F., Oosterloo, T., Adams, E. A. K., Oman, K.A. & Leisman, L. 2021, MNRAS, in press (arXiv:2112:00017)
 McGaugh S.S., 2009, ApJ, **632**, 854
 Milgrom M. 1983, ApJ, **270**, 365
 Miller, R. H., Prendergast K. H. & Quirk, W. 1971, ApJ, **161**, 903
 Moreno, J., Danieli, S., Bullock, J. S., *et al.* 2022, arXiv:2202.05836
 Ostriker, J. P. & Peebles, P. J. E. 1973, ApJ, **186**, 467-80
 Read, J. I., Agertz, O. & Collins, M. L. M. 2016, MNRAS, **459**, 2573
 Sanders, R. H. 2010, *The Dark Matter Problem: A Historical Perspective* (Chap. 3) (Cambridge University Press)

- Sellwood, J. A. 2014, arXiv:1406.6606 (on-line manual: <http://www.physics.rutgers.edu/~sellwood/manual.pdf>)
 Sellwood, J. A. 2016, ApJ, **819**, 92
 Sellwood, J. A., Shen, J. & Li, Z. 2019, MNRAS, **486**, 4710
 Shu, F. H. 1969, ApJ, **158**, 505
 Somerville, R. S. & Davé, R. 2015, ARA&A, **53**, 51-113
 Springel, V. 2005, MNRAS, **364**, 1105
 Tamburro, D., Rix, H.-W., Leroy, A. K., *et al.* 2009, AJ, **137**, 4424
 Toomre, A. 1963, ApJ, **138**, 385
 Toomre, A. 1964, ApJ, **139**, 1217
 Toomre, A. 1981, In *The Structure and Evolution of Normal Galaxies*, eds. S. M. Fall & D. Lynden-Bell (Cambridge, Cambridge Univ. Press) p. 111
 van Dokkum, P., Danieli, S., Abraham, R., *et al.* 2019, ApJ, **874**, L5

This paper has been typeset from a $\text{\TeX}/\text{\LaTeX}$ file prepared by the author.